Occurrence of kornerupine-bearing granulite from Kunjan locality, Salem district, Tamil Nadu, India

D. Prakash[1,*], C. K. Singh[1], R. S. Kumar[2], R. Yadav[1], S. K. Rai[1], M. K. Yadav[3], Pradip K. Singh[1] and S. Jaiswal[1]

[1]Centre of Advanced Study in Geology, Banaras Hindu University, Varanasi 221 005, India
[2]Department of Earth Sciences, Annamalai University, Annamalai Nagar 608 002, India
[3]Centre of Advanced Study in Geology, University of Lucknow, Lucknow 226 007, India

Kornerupine, although a rare mineral, has been reported from several locations around the world in various types of aluminomagnesian Proterozoic rocks subjected to amphibolite and granulite facies metamorphism. Here we report the occurrence of kornerupine in quartzo-feldspathic gneisses near Kunjan town located in the southwestern part of Salem district, Tamil Nadu, India. These kornerupine granulites show well-preserved retrogression texture, involving hydration reactions which helped develop the various mineral assemblages. The common stable assemblage in these granulites is orthopyroxene–cordierite–kornerupine–biotite–spinel–K-feldspar–plagioclase. The *P–T* conditions of these granulites have been derived using the *win*TWQ program, which gives results of ~800°C and ~6 kbar for kornerupine-bearing assemblage. The high *P–T* assemblage reported from this area bears a significant relationship with the metamorphic history and exhumation of the Salem–Namakkal block.

Keywords: Hydration reactions, kornerupine granulites, metamorphic evolution, mineral assemblages, retrogression texture.

KORNERUPINE [(Cl, Mg, Fe^{2+}, Na) (Mg, Fe^{2+})$_3$ (Al, Mg, Fe^{3+})$_6$ (Si, Al, B)$_5O_{21}$ (O, OH, F)] is a complex borosilicate mineral[1] characterized by an orthorhombic–dipyramidal crystal structure[2] with most of the naturally occurring kornerupines containing up to 4 wt.% of B_2O_3 (ref. 3). The variable composition may impart kornerupine its colour ranging from colourless to yellow, green, brown, etc.[4,5]. Though kornerupine is an uncommon mineral, it has been reported from more than 70 locations worldwide, including India, in various Mg–Al-rich amphibolite and granulite facies Proterozoic rocks[6,7]. Many of the boron-free kornerupines have been reported from the Al-rich lenses occurring within or in close association with the anorthosites, such as from the Messina Layered Intrusion, southern Africa[8,9]; Fiskenæsset Harbour, Greenland[10,11] and Reynolds Range, central Australia[12,13]. In India, kornerupine was first reported by Murthy[14] from the biotite gneisses of the Dudhi region, Uttar Pradesh. Later, Balasubrahmanyan[15] reported the presence of kornerupine from the sapphirine-bearing granulites of Kovilpatti area, Madras (now Chennai) and Lal *et al.*[16], reported this rare mineral from sapphirine-bearing granulites of the Sonapahar area, Assam. Subsequently, Grew[17] identified five kornerupine-bearing granulite localities from the Southern Granulite belt and the Eastern Ghats belt. Recently, Sajeev *et al.*[18] reported kornerupine from the granulites of Ganguvarpatti village, Tamil Nadu, and Sharma and Prakash[19] reported its occurrence in the sapphirine-free granulites of Karimnagar area, Andhra Pradesh. The present study reports the occurrence of kornerupine from Kunjan locality, southwest Salem district, Tamil Nadu.

Based on the divergent lithology, metamorphic grades and radiometric ages, the Southern Granulite Terrain (SGT) of India has been divided from north to south into several tectonic blocks[20,21], viz. Salem block, Namakkal block, Madurai block, Trivandrum block and Nagercoil block (Figure 1 *a*). The Kunjan locality is a part of SGT and lies in the Salem–Attur Shear Zone (SASZ) to the southwest of the Salem block (Figure 1 *b*). Previous workers have noted different episodes of granulite facies metamorphism at different geological intervals in SGT, such as at 2.5 Ga (refs 22–25), 0.7 Ga (ref. 26) and 0.6 Ga (refs 27–29). It has also been deduced that the Salem block represents the southward extended part of the Dharwar craton, where the cratonic rocks have got metamorphosed into granulite facies[30–34]. In the Salem block, the Archean and Paleoproterozoic rocks are characterized by contrasting lithological characters[35]. The isolated hillocks in Salem block consist dominantly of quartz–feldspar gneisses, basic granulites, charnockites and banded iron formations of Meso-Neoarchaean age. The comparatively younger basic and acidic intrusives are Neo-Proterozoic in age. The Quaternary rocks, represented by Kankar/calcretes, overlie unconformably to these crystalline rocks. Structurally, the area has experienced polyphase deformational episodes. At least three phases of folds followed by faults and shears developed through brittle and ductile deformations on a regional scale[34]. The SASZ dominantly consists of orthogneisses and quartz–feldspar gneisses as country rocks with the other rock types such as amphibolites, charnockites and mafic granulites occurring intermittently in the hillocks[34,36]. The kornerupine granulite occurs as a thin layer in association with the biotite-bearing quartzo-feldspathic gneisses (Figure 2 *a* and *c*). The rock containing kornerupine is massive, coarse-grained and dark- to light-coloured in appearance. It has an inequigranular granoblastic texture (Figure 2 *b* and *d*). The layer exposed is partially weathered and field relationships with quartzo-feldspathic gneisses are obscure due to extensive laterization (Figure 2 *a* and *c*).

The important assemblage in the kornerupine-bearing granulite includes kornerupine–cordierite–biotite–spinel–orthopyroxene–K-feldspar–plagioclase. Kornerupine is dark

*For correspondence. (e-mail: dprakashbhu@gmail.com)

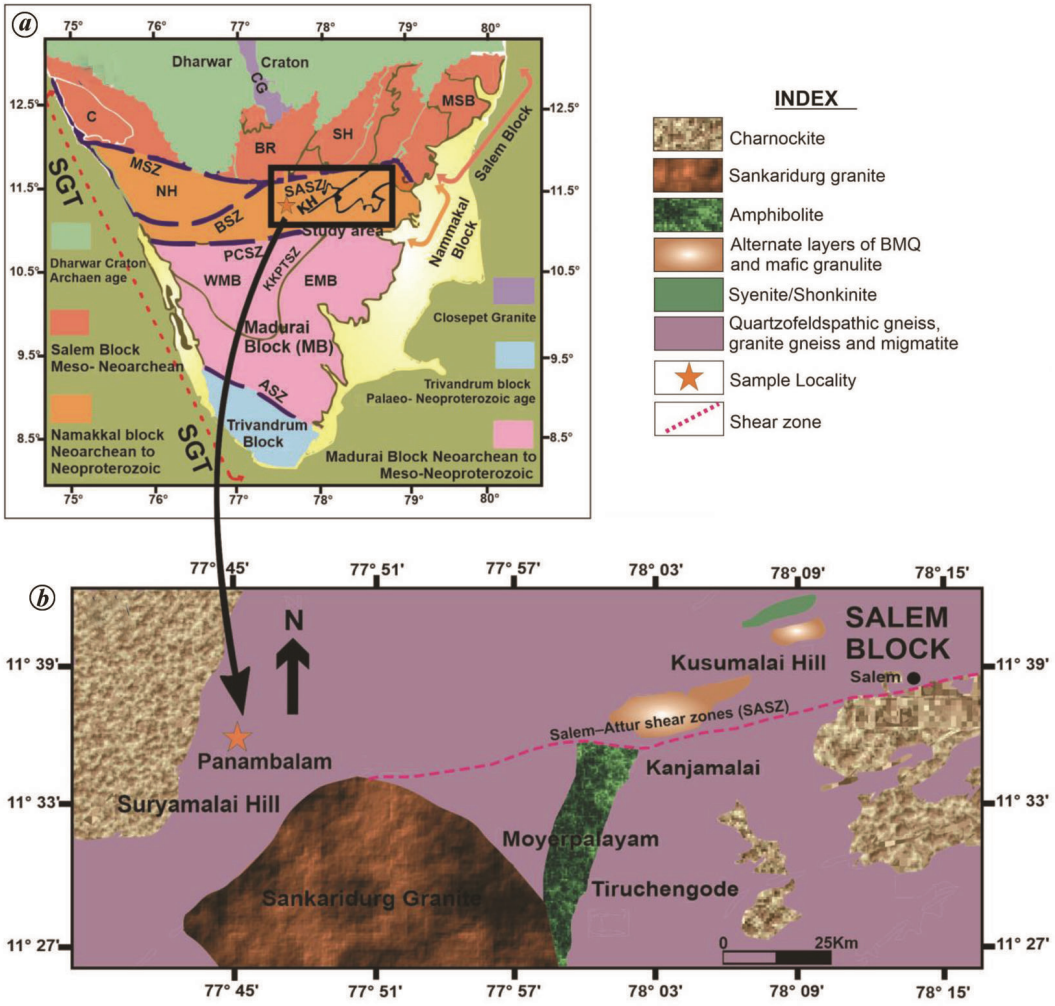

Figure 1. ***a***, Map of southern India showing major shear zones (dashed lines). ASZ, Achankovil shear zone; BR, Biligirirangan; BSZ, Bhabani shear zone; C, Coorg; CG, Closepet granite; EDC, Eastern Dharwar craton; WDC, Western Dharwar craton; FL, Fermor's line; KH, Koli hill; KKPTSZ, Karur–Kambam–Painavu–Trichur shear zone; MSB, Madras block; MSZ, Moyar shear zone; SH, Shevroy hill; PCSZ, Palghat Cauvery shear zone; SASZ, Salem–Attur shear zone (modified after Behera *et al.*[34]). ***b***, Geological map of the Salem–Namakkal block (modified after Behera *et al.*[34]).

green in colour, weakly pleochroic, coarse-grained, prismatic, idioblastic to sub-idioblastic, and constitutes up to 40% of the rock along with biotite (20%) and cordierite (20%) (Figure 2 *b* and *d*). Spinel, orthopyroxene and cordierite occur as inclusions within kornerupine (Figure 3 *a*), according to the following reaction:

$$\text{Spinel} + \text{orthopyroxene} + \text{cordierite} + H_2O = \text{kornerupine}. \quad (1)$$

The intergrowth of biotite and kornerupine involves a biotite-producing reaction at the expense of orthopyroxene and spinel (Figure 3 *b*). Orthopyroxene porphyroblasts occur along with these intergrowths (Figure 3 *b*). Spinel inclusions in kornerupine are nowhere found to be in direct contact with biotite. Kornerupine may have been formed as a result of the following reaction:

$$\text{Orthopyroxene} + \text{spinel} + H_2O = \text{Biotite} + \text{kornerupine} + \text{K-feldspar}. \quad (2)$$

Kornerupine formation is a localized product during retrogression. Therefore, both spinel and orthopyroxene may be the peak metamorphic mineral paragenesis present as relict within kornerupine.

The constituent minerals of kornerupine-bearing granulite were analysed using GEOLJXA-8800L electron microprobe analyser (EPMA) at the University of Wurzburg, Germany, with beam current of 5 ηA at an accelerating voltage of 15 kV. Table 1 gives representative probe data of various minerals.

Orthopyroxenes in the analysed samples were found to be extremely rich in iron and magnesium, and contained small amounts of MnO, CaO, TiO_2 and Na_2O. The cation totals on the basis of six-oxygen atoms per formula unit

were close to 4, which implies that Fe^{3+} is not present in orthopyroxene. Distinct compositional zoning was absent in the prismatic orthopyroxene and the maximum X_{Mg} ranged from 0.717 at the core to 0.706 at the rim. The

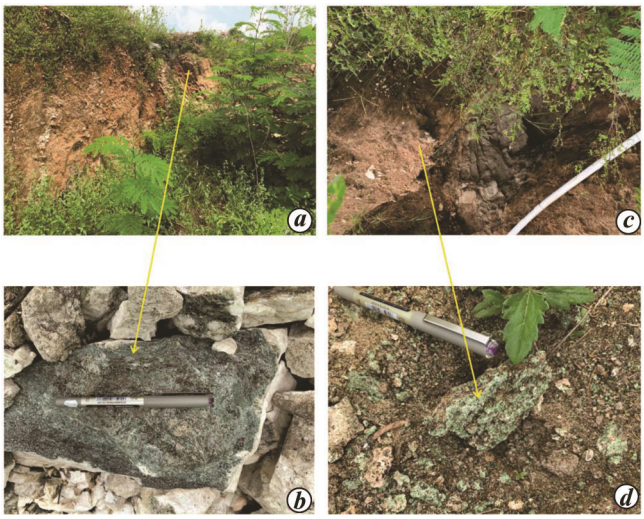

Figure 2. ***a***, Exposure of quartzo-feldspathic gneisses near Panambalam village, Edapadi, Salem, Tamil Nadu, showing sample location (yellow arrow). Photograph is an incline shot as it is an abandoned old mine work; the narrow opening is 4′ × 5′. It shows the eastern vertical wall of the old working. The exposed vertical surface is about 11 ft. ***b***, Greenish-blue kornerupine by bearing quartzo-feldspathic gneisses (length of the pen is 12.6 cm). Photograph shows the leftout waste material with some samples having kornerupine and biotite. ***c***, Kornerupine-bearing rock occurring as patches within the quarzo-feldspathic gneisses near Kunjan locality, Edapadi, Salem showing sample location (yellow arrow). ***d***, Mesoscopic, greenish-blue-coloured crystals of kornerupine in quartzo-feldspathic gneisses (length of the pen is 12.6 cm). Photograph shows *in situ* weathered sample; this part of the rock is seen exposed at the old work site itself.

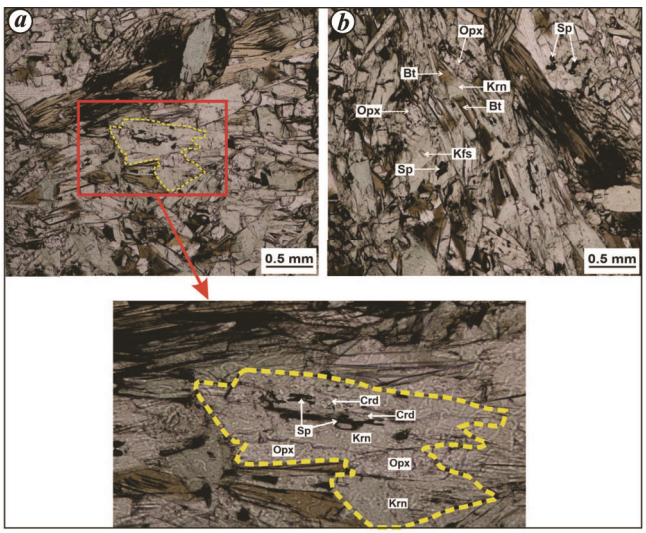

Figure 3. ***a***, Photomicrograph of kornerupine-bearing quartz-free granulite showing fractured megacryst of kornerupine having prominent inclusion of spinel, orthopyroxene and cordierite. ***b***, Photomicrograph showing intergrowth of kornerupine and biotite, whereas spinel and orthopyroxene are isolated from each-other. Krn, Kornerupine; Opx, Orthopyroxene; Crd, Cordierite; Spl, Spinel; Bt, Biotite and Kfs, Potash feldspar.

sum of anhydrous oxides in cordierite was less than 100%, which apparently suggests that cordierite contains fluid phases in the structural channels[37–39]. X_{Mg} in cordierite ranged from 0.905 at the core to 0.869 at the rim. Although kornerupine is a borosilicate mineral, no boron was found in the present analyses. The analysed data of kornerupine were plotted on the (Fe^{2+}, Mn, Mg)O–(Al, Cr, Fe^{3+})O_3–SiO_2 diagram (Figure 4 *a*). The composition of the analysed kornerupine lay on the solid solution join between $4MgO–3Al_2O_3–4SiO_2$ (4 : 3 : 4) composition and $3.5MgO.3.5Al_2O_3.3.5SiO_2$ (1 : 1 : 1) composition. An appreciable amount of Fe^{2+} was observed that ranged from 0.830 at the core to 0.951 at the rim. X_{Mg} ranged from 0.777 at the core to 0.756 at the rim. X_{Mg} biotite ranged from 0.718 (core) to 0.694 (rim). Ti content in biotite showed a remarkably narrow range, i.e. 0.535 (core)–0.514 (rim) pfu. Spinel was largely Mg-rich with X_{Mg} ranging from 0.560 to 0.557 from core to rim. Plagioclase did not show zoning and the analysed matrix gave a maximum X_{An} of 0.456, whereas the phase of potassium feldspar showed a maximum value of X_{Or} = 0.957.

The ternary FMAS diagram (Fe^{2+}, Mg)O–Al_2O_3–SiO_2 was used to represent the mineral paragenesis associated with kornerupine and the reactions involved in its formation (Figure 4 *b*). The minerals whose compositions have been plotted in this diagram include kornerupine, orthopyroxene, cordierite, spinel and biotite. The voluminous late-stage biotite in kornerupine–granulite may be the result of hydrous retrogression caused due to potash-rich fluid influx from the adjacent high-grade gneisses, when the partial melts in these gneisses, started crystallizing and released hydrous fluids[40,41].

The *P–T* condition for the formation of kornerupine-bearing granulites was derived employing *win*TWQ, which is an internally consistent program (version 2.32)[42] which uses the thermodynamic datasets of Berman[43], Berman *et al.*[44], and Aranovich and Berman[45], considering the phases enstatite, cordierite, Fe-cordierite, eastonite, ferrosilite, phlogopite, annite, spinel and β-quartz of the end-members. Nine possible equilibria were obtained for the selected phases of the end-members (Table 2). Core compositions for sample no. 5698 using these equilibria, gave an intersection at 800°C and 6 kbar (Figure 5 *a*). These pressure and temperature estimates obtained for kornerupine-bearing granulites certainly do not represent the peak metamorphic condition of the area, but the post-peak conditions of granulite-facies metamorphism[46].

Mukhopadhyay and Bose[47] estimated *P–T* conditions for the assemblage garnet–orthopyroxene–clinopyroxene–plagioclase in the mafic granulites of the Salem block to be 8–14 kbar/875–900°C. Santosh *et al.*[46] on the basis of detailed petrography and phase equilibria studies of the garnet–clinopyroxene-bearing mafic rocks (lacking omphacite and containing minor amounts of plagioclase, orthopyroxene and quartz) of the Salem block, suggested that the area must have experienced a high to ultrahigh-temperature

Table 1. Representative microprobe analyses of the coexisting minerals in Kornerupine-bearing granulite (sample no. 5698)

Spot no. →	I	I	II	II	III	III	IV	IV	V	V	VI	VI
Minerals →	Ortho-pyroxene	Ortho-pyroxene	Cordierite	Cordierite	Kornerupine	Kornerupine	Biotite	Biotite	Spinel	Spinel	K-feldspar	Plagioclase
Oxides ↓	Core	Rim	Core	Rim	Core	Rim	Core	Rim	Core	Rim	Matrix	Matrix
SiO_2	50.90	49.94	50.10	49.23	28.88	28.76	38.26	38.03	0.00	0.00	64.14	64.91
TiO_2	0.02	0.00	0.00	0.00	0.07	0.34	4.88	4.67	0.00	0.00	0.00	0.19
Al_2O_3	6.95	7.98	32.91	33.92	43.34	42.34	15.91	15.98	63.93	64.01	18.89	20.78
Cr_2O_3	0.00	0.00	0.00	0.00	0.00	0.00	0.00	0.38	0.00	0.09	0.00	0.18
FeO	17.05	17.86	3.01	3.02	7.81	8.92	11.09	11.98	21.25	21.45	0.00	0.03
MnO	0.00	0.00	0.29	0.27	0.14	0.13	0.00	0.00	0.00	0.00	0.00	0.20
MgO	24.23	24.08	12.01	11.22	15.23	15.52	15.87	15.23	14.03	14.01	0.00	0.00
CaO	0.23	0.00	0.00	0.00	0.52	0.48	0.19	0.00	0.00	0.00	0.18	1.63
Na_2O	0.19	0.10	0.00	0.18	0.58	0.53	0.27	0.09	0.00	0.00	0.36	7.42
K_2O	0.00	0.00	0.00	0.00	0.54	0.28	8.92	8.98	0.00	0.00	15.58	5.02
Total	99.57	99.96	98.23	97.84	97.11	97.3	95.39	95.34	99.21	99.56	99.15	100.36
O	6	6	18	18	21	21	22	22	4	4	8	8
Si	1.852	1.817	5.037	4.976	3.669	3.665	5.572	5.566	0.000	0.000	2.981	2.895
Ti	0.001	0.000	0.000	0.000	0.007	0.033	0.535	0.514	0.000	0.000	0.000	0.006
Al	0.298	0.342	3.900	4.041	6.489	6.359	2.730	2.756	1.966	1.963	1.035	1.092
Cr	0.000	0.000	0.000	0.000	0.000	0.000	0.000	0.044	0.000	0.002	0.000	0.006
Fe^{2+}	0.519	0.543	0.189	0.255	0.830	0.951	1.350	1.466	0.429	0.432	0.000	0.001
Fe^{3+}	0.000	0.000	0.064	0.000	0.000	0.000	0.000	0.000	0.034	0.035	0.000	
Mn	0.000	0.000	0.025	0.023	0.015	0.014	0.000	0.000	0.000	0.000	0.000	0.008
Mg	1.314	1.306	1.799	1.690	2.885	2.949	3.445	3.323	0.545	0.543	0.000	0.000
Ca	0.009	0.000	0.000	0.000	0.071	0.066	0.030	0.000	0.000	0.000	0.009	0.078
Na	0.013	0.007	0.000	0.035	0.143	0.131	0.076	0.026	0.000	0.000	0.032	0.642
K	0.000	0.000	0.000	0.000	0.088	0.046	1.657	1.676	0.000	0.000	0.924	0.286
X_{Mg}	0.717	0.706	0.905	0.869	0.777	0.756	0.718	0.694	0.560	0.557	$X_{Or} = 0.957$	$X_{An} = 0.456$

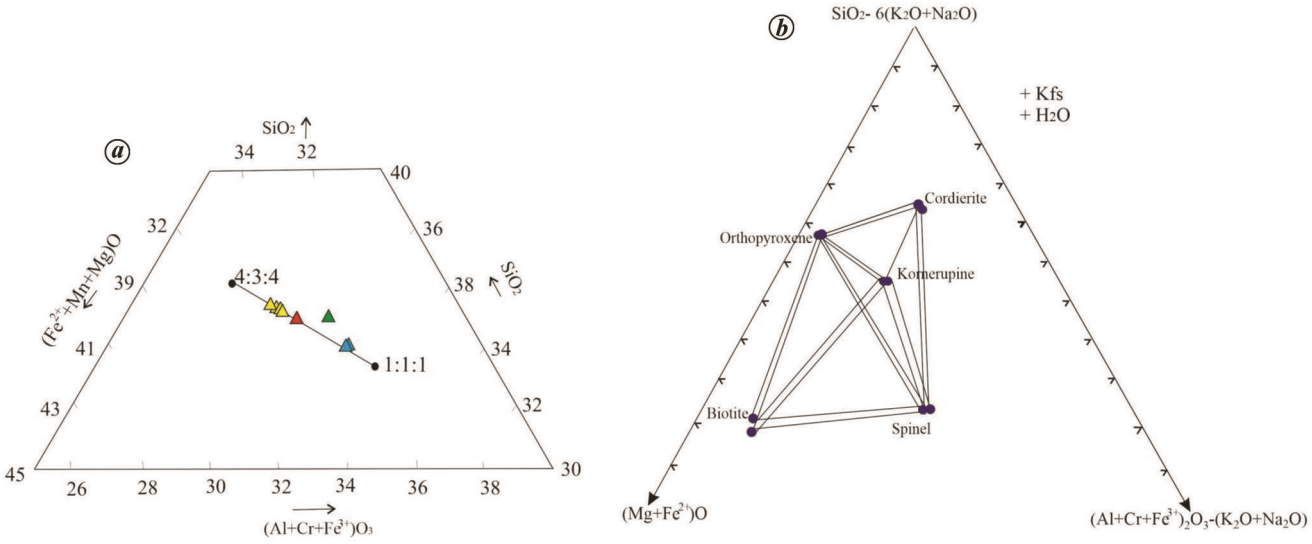

Figure 4. ***a***, $(Fe^{2+}, Mg)O–Al_2O_3–SiO_2$ triangular plot showing composition of kornerupine. Yellow triangle indicates composition of kornerupine from the study area. Red triangle (Ellammankovilpatti), green triangle (Ganguvarpatti) and blue triangle (Ponakkadu) are kornerupine composition plots from Grew[9] for comparison. ***b***, Topological configuration kornerupine-bearing granulites in the $[(SiO_2–6K_2O–6Na_2O)]–[(Fe,Mg)O]–[(Al,Cr,Fe^{3+})_2O_3–K_2O–Na_2O)]$ diagram projected from K-feldspar. Solid circles represent compositional plot of kornerupine and associated minerals.

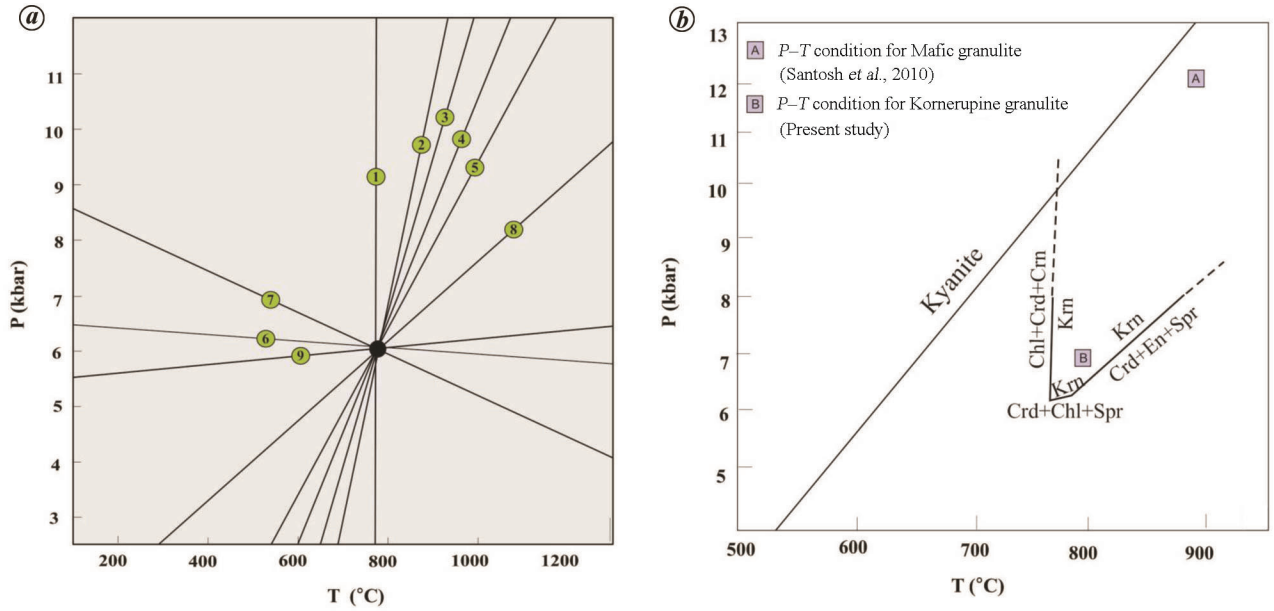

Figure 5. ***a***, Simultaneous calculations of pressure and temperature conditions using *win*TWQ program for core composition. ***b***, Stability field for boron-free kornerupine in the kyanite–sillimanite phase diagram together with *P–T* estimates of the Kunjan area, Salem.

metamorphism, followed by an isothermal decompression stage[46]. The phase equilibria modelling for garnet–clinopyroxene-bearing retrogressed eclogites at Sittampundi (having relict omphacite) yielded peak *P–T* conditions of 1010°C and 19 kbar. The result is also supported by the conventional geothermobarometry of the mafic granulites from Perundarai area in the Salem block. However, geothermobarometric studies of mafic rocks from the nearby Kanji Malai yielded values as low as 7.4 kbar and 750°C, which suggests that the rocks in this area have undergone a retrograde metamorphic stage which has strongly overprinted its peak metamorphic history[46].

Lack of suitable geothermobarometers associated with the prograde metamorphism poses limitation in estimation of peak *P–T* conditions for the kornerupine granulite. However, the *P–T* estimations from mafic rocks in the area reported by previous workers indicate that the peak metamorphism in the studied area must have occurred at >900°C and >10 kbar (ref. 46) (Figure 5 *b*), as is also evident from the presence of spinel and orthopyroxene as

Table 2. Simultaneous calculation of *P–T* conditions using *win*TWQ program (version 2.32)

Reaction	ΔS (J/K^{-1})	ΔV (Jbar^{-1})
fCd + Phl = Sp + 4 bQz + 2 Fsl + Eas	–42.597	–3.881
2 fCd + 2 Phl = 3 bQz + 4 Fsl + 2 Eas + Cd	–50.121	–4.257
2 Ann + 7 bQz + 4 Sp = 4 Fsl + fCd + 2 Eas	7.734	2.88
6 Eas + 12 Fsl + 9 bQz = 2 Phl + 3 Cd + 4 Ann	174.94	12.517
4 Cd + 5 Eas + 10 Fsl = 3 Sp + 5 Phl + 5 fCd	72.692	5.385
Cd + 2 Fsl = fCd +2 En	1.02	0.20
2 Fsl + 5 bQz + 2 Sp = fCd +2 En	1.34	0.15
5 bQz + 2 Sp = Cd	35.074	3.505
Eas + 3 Fsl = Sp + bQz + En + Ann	0.58	0.02

Phases used in the calculation: Sp, Spinel; Eas, Eastonite; Phl, Phlogopite; Ann, Annite; Fsl, Ferrosilite; En, Enstatite; fCd, Fe cordierite; Cd, Cordierite; bQz, Beta-quartz.
ΔS and ΔV calculated at 1 bar and 298 K (sample no. 5698).

inclusions within retrograded kornerupine. Partial hydration favouring growth of kornerupine subsequent to peak metamorphism was evident from the partial replacement of orthopyroxene–spinel by biotite and kornerupine (Figure 3 *b*).

Layers of kornerupine-bearing assemblages occurred within high-grade granulite facies rocks in the study area. However, the *P–T* estimates obtained using *win*TWQ for these assemblages were ~800°C and ~6 kbar, which indicates that boron-free kornerupine can occur at lower temperatures and pressures. The stability field for boron-free kornerupine shown in Figure 5 *b* indicates that it is stable at higher *P–T* than obtained in the present study[48]. The *P–T* stability field for boron-bearing kornerupine is not well-established[49], but the hydrothermal replacement of tourmaline by kornerupine occurs at ~950°C and 5 kbar (ref. 50). Thus, the *P–T* conditions estimated for the formation of boron-free kornerupine in the FMAS diagram must be considered lower than that would be obtained for boron-bearing Kornerupine.

The biotite-bearing quartzofeldspathic paragneiss that hosts kornerupine is widespread and abundant in Kunjan and adjacent areas. Similar occurrences in the world hosted by aluminous paragneisses have been reported from Canada, Australia, Madagascar, Antarctica and also other parts of India. Kornerupine is a rare mineral and has been reported so far from nearly 75 localities worldwide. The occurrences reported are from granulite as well as upper amphibolite facies metamorphic complexes of Precambrian age[51]. Kornerupine is usually formed from the breakdown of tourmaline during prograde metamorphism or in anatectic melts, but some reports suggest the role of boron metasomatism in the formation of kornerupine[51]. It most commonly occurs in silica-deficient, Al–Mg-rich rocks, but boron-rich members may occur in more diverse chemical environments. Mg–Al-rich granulites are although not abundant, but commonly found in high-grade terranes like SGT, EGB, CITZ, etc. around the world, but due to absence of the above required composition, kornerupine is rarely formed along with these Mg–Al granulites. In the present study, kornerupine is inferred to have formed at late stage of mineral growth, but in many samples it is found to be closely associated with high-grade minerals. The minerals, remnant of thermal peak, are spinel and orthopyroxene. The formation of kornerupine may have taken place at or shortly after peak stage of metamorphism, associated with higher water activity, in the presence of excess fluids and at somewhat lower thermal conditions than those of high-grade minerals. This is evident from its coarse, idioblastic crystals formed at late stage and found to be associated with other water/volatile-bearing minerals. Orthopyroxene–spinel pair partially replaced by biotite and kornerupine well documents this post-peak retrograde hydration stage (Figure 3 *b*). The K_2O influx during this retrogression might have promoted the high growth of late-stage biotite. As a concluding remark, the outcomes of the present study generate scope for further petrological, mineralogical and isotopic works on the occurrences of natural kornerupines, particularly with regard to their mineral paragenesis and metamorphic evolution of the Salem block.

1. Moore, P. B. and Bennett, J. B., Kornerupine: its crystal structure. *Science*, 1968, **159**, 524–526.
2. Grew, E. S., Cooper, M. A. and Howthorne, F. C., Prismatine: revalidation for boron-rich compositions in the kornerupine group. *Mineral. Mag.*, 1996, **60**, 483–491.
3. Grew, E. S., Chernosky, J. V., Werding, G., Abraham, K., Marquez, N. and Hinthorne, J. R., Chemistry of kornerupine and associated minerals, a wet chemical, ion microprobe, and X-ray study emphasizing Li, Be, B and F contents. *J. Petrol.*, 1990, **31**, 1025–1070.
4. Carson, C. J., Hand, M. and Dirks, P. H. G. M., Stable coexistence of grandidierite and kornerupine during medium pressure granulite facies metamorphism. *Mineral. Mag.*, 1995, **59**, 327–339.
5. Young, D. A., Kornerupine-group minerals in Grenville granulite-facies paragneiss, Reading Prong, New Jersey. *Can. Mineral.*, 1995, **33**, 1255–1262.
6. Prakash, D. and Sharma, I. N., Metamorphic evolution of Karimnagar Granulite Terrane, Eastern Dharwar craton, South India. *Geol. Mag.*, 2011, **148**(1), 112–132.
7. Prakash, D., Singh, P. C., Tewari, S., Joshi, M., Frimmel, H. E., Hokada, T. and Rakotonandrasana, T., Petrology, pseudosection modelling and U–Pb geochronology of silica-deficient Mg–Al granulites from the Jagtiyal section of Karimnagar Granulite terrane, Northeastern Dharwar craton, India. *Precambrian Res.*, 2017, **299**, 177–194.

8. Windley, B. F., Ackermand, D. and Herd, R. K., Sapphirine/kornerupine-bearing rocks and crustal uplift history of the Limpopo belt, Southern Africa. *Contrib. Mineral. Petrol.*, 1984, **86**, 342–358.
9. Klaska, R. and Grew, E. S., The crystal structure of B-free kornerupine: conditions favoring the incorporation of variable amounts of B through $^{[4]}$BÅ ⇌ $^{[4]}$Si substitution in kornerupine. *Am. Mineral.*, 1991, **76**(11–12), 1824–1835.
10. Herd, R. K., Sapphirine and kornerupine occurrences within the Fiskenaesset complex. *Rapport Grønlands Geologiske Undersøgelse*, 1973, **51**, 65–71.
11. Schreyer, W. and Abraham, K., Natural boron-free kornerupine and its breakdown products in a sapphirine rock of the Limpopo Belt, southern Africa. *Contrib. Mineral. Petrol.*, 1976, **54**(2), 109–126.
12. Vry, J. K. and Cartwright, I., Sapphirine–kornerupine rocks from the Reynolds Range, central Australia: constraints on the uplift history of a Proterozoic low pressure terrain. *Contrib. Mineral. Petrol.*, 1994, **116**(1), 78–91.
13. Friend, C. R. L., Occurrences of boron-free and boron-poor kornerupine. *Mineral. Mag.*, 1995, **59**(394), 163–166.
14. Murthy, M. V. N., Kornerupine from Rannu, Uttar Pradesh. *Nature*, 1954, **174**, 1065.
15. Balasubrahmanyan, M. N., Note on kornerupine from Ellammankovilpatti, Madras. *Mineral. Mag.*, 1965, **35**, 662–664.
16. Lal, R. K., Ackermand, D., Seifert, F. and Haldar, S. K., Chemographic relationships in sapphirine-bearing rocks from Sonapahar, Assam, India. *Contrib. Mineral. Petrol.*, 1978, **67**, 169–187.
17. Grew, E. S., Sapphirine, kornerupine and sillimanite + orthopyroxene in the charnockitic region of South India. *J. Geol. Soc. India*, 1982, **23**, 469–505.
18. Sajeev, K., Osanai, Y. and Santosh, M., Ultrahigh-temperature metamorphism followed by two-stage decompression of garnet–orthopyroxene–sillimanite granulites from Ganguvarpatti, Madurai block, southern India. *Contrib. Mineral. Petrol.*, 2004, **148**, 29–46.
19. Sharma, I. N. and Prakash, D., New occurrence of kornerupine-bearing granulites from Karimnagar, Andhra Pradesh. *Curr. Sci.*, 2006, **91**, 678–683.
20. Santosh, M., Maruyama, S. and Sato, K., Anatomy of a Cambrian suture in Gondwana: Pacific type orogeny in southern India? *Gondwana Res.*, 2009, **16**, 321–341.
21. Santosh, M., Tsunogae, T., Tsutsumi, Y. and Iwamura, M., Microstructurally controlled monazite chronology of ultrahigh-temperature granulites from southern India: Implications for the timing of Gondwana assembly. *Island Arc*, 2009, **18**(2), 248–265.
22. Peucat, J. J., Mahabaleswar, B. and Jayananda, M., Age of younger tonalitic magmatism and granulitic metamorphism in the South Indian transition zone (Krishnagiri area); comparison with older Peninsular gneisses from the Gorur–Hassan area. *J. Metamorph. Geol.*, 1993, **11**(6), 879–888.
23. Prakash, D., New SHRIMP U–Pb zircon ages of the metapelitic granulites from NW of Madurai, South India. *J. Geol. Soc. India*, 2010, **76**, 371–383.
24. Sato, K., Santosh, M., Tsunogae, T., Chetty, T. R. K. and Hirata, T., Laser ablation ICP mass spectrometry for zircon U–Pb geochronology of metamorphosed granite from the Salem block: implication for Neoarchean crustal evolution in southern India. *J. Mineral. Petrol. Sci.*, 2011, **106**, 1–12.
25. Anderson, J.R., Payne Justin, L., Kelsey David, E., Hand, M., Collins Alan, S. and Santosh, M., High-pressure granulites at the dawn of the Proterozoic. *Geology*, 2012, **40**(5), 431–434.
26. Rao, Y. J., Chetty, T. R. K., Janardhan, A. S. and Gopalan, K., Sm–Nd and Rb–Sr ages and *P–T* history of the Archean Sittampundi and Bhavani layered meta-anorthosite complexes in Cauvery shear zone, South India: evidence for Neoproterozoic reworking of Archean crust. *Contrib. Mineral. Petrol.*, 1996, **125**(2), 237–250.
27. Prakash, D., Yadav, R., Tewari, S., Frimmel, H. E., Koglin, N., Sachan, H. K. and Yadav, M. K., Geochronology and phase equilibria modelling of ultra-high temperature sapphirine + quartz-bearing granulite at Usilampatti, Madurai Block, Southern India. *Geol. J.*, 2018, **53**(1), 139–158.
28. Bhutani, R., Balakrishnan, S., Nevin, C. G. and Jeyabal, S., Sm–Nd isochron ages from Southern Granulite Terrain, South India: age of protolith and metamorphism. *Geochem. Cosmochim. Acta*, 2007, **71**(15), A89.
29. Tewari, S., Prakash, D., Yadav, M. K. and Yadav, R., Petrology and isotopic evolution of granulites from central Madurai Block (southern India): reference to Ediacaran crustal evolution. *Int. Geol. Rev.*, 2018, **60,** 1791–1815.
30. Friend, C. R. L. and Nutman, A. P., Response of zircon U–Pb isotopes and whole-rock geochemistry to CO_2 fluid-induced granulite-facies metamorphism, Kabbaldurga, Karnataka, South India. *Contrib. Mineral. Petrol.*, 1992, **111**(3), 299–310.
31. Bartlett, J. M., Dougherty-Page, J. S., Hams, N. B. W., Hawksworth, C. J. and Santosh, M., The application of single zircon evaporation and model Nd ages to the interpretation of polymetamorphic terrains: an example from the Proterozoic mobile belt of South India. *Contrib. Mineral. Petrol.*, 1998, **131**, 181–195.
32. Bhaskar Rao, Y. J., Janardhan, A. S., Kumar, T., Narayana, B. L., Dayal, A. M., Taylor, P. N. and Chetty, T. R. K., Sm–Nd model ages and Rb–Sr isotopic systematics of charnockites and gneisses across the Cauvery shear zone of southern India: implications for the Archean–Neoproterozoic terrain boundary in the Southern Granulite Terrain. *Mem. Geol. Soc. India*, 2003, **50**, 434.
33. Ghosh, J. G., De Wit, M. J. and Zartman, R. E., Age and tectonic evolution of Neoproterozoic ductile shear zones in the Southern Granulite Terrain of India, with implications for Gondwana studies. *Tectonics*, 2004, **23**, TC3006.
34. Behera, B. M., Waele, B. D., Thirukumar, V., Sundaralingam, K., Narayanana, S., Sivalingam, B. and Biswal, T. K., Kinematics, strain pattern and geochronology of the Salem–Attur shear zone: tectonic implications for the multiple sheared Salem–Namakkal blocks of the Southern Granulite Terrane, India. *Precambrian Res.*, 2019, **324**, 32–61.
35. Subramanian, K. S. and Selvan, T. A., *Geology of Tamil Nadu and Pondicherry*, Geological Survey of India, Bengaluru, India, 2001, p. 192; http://www.geosocindia.org/index.php/bgsi/article/view/55854
36. Sundaralingam, K., Biswal, T. K. and Thirukumaran, V., Strain analysis of the Salem–Attur shear zone of Southern Granulite Terrane around Salem, Tamil Nadu. *J. Geol. Soc. India*, 2017, **89**(1), 5–11.
37. Armbruster, T. and Bloss, F. D., Mg-cordierite: Si/Al ordering, optical properties, and distortion. *Contrib. Mineral. Petrol.*, 1981, **77,** 332–336.
38. Santosh, M., Jackson, D. H. and Harris, N. B. W., The significance of channel and fluid inclusion CO_2 in cordierite: evidence from carbon isotopes. *J. Petrol.*, 1993, **34**, 233–258.
39. Prakash, D., Petrology of the basic granulites from Kodaikanal, South India. *Gondwana Research*, 1999, **2**, 95–104; https://www.sciencedirect.com/science/article/abs/pii/S1342937X05701301
40. Hensen, B. J. and Warren, R. G., Partial melting during granulite metamorphism, a mechanism for control of fluid composition? In IGCP Project 236. Precambrian Events in the Gondwana Fragments, Conference and Field Excursion, 1985, pp. 69–70.
41. Goscombe, B., Silica-undersaturated sapphirine, spinel and kornerupine granulite facies rocks, NE Strangways Range, Central Australia. *J. Met. Geol.*, 1992, **10**, 181–201.
42. Berman, R. G., *win*TWQ (version 2.3): a software package for performing internally-consistent thermobarometric calculations. Geological Survey of Canada, Open File 5462. ed. 2.32, 2007, p. 41.
43. Berman, R. G., Internally consistent thermodynamic data for stoichiometric minerals in the system Na_2O–K_2O–CaO–FeO–Fe_2O_3–Al_2O_3–SiO_2–TiO_2–H_2O–CO_2. *J. Petrol.*, 1988, **29**, 445–522.

44. Berman, R. G., Aranovich, L. Y. and Pattison, D. R. M., Reassessment of the garnet–clinopyroxene Fe–Mg exchange thermometer: II. Thermodynamic analysis. *Contrib. Mineral. Petrol.*, 1995, **119**, 30–42.
45. Aranovich, L. Y. and Berman, R. G., A new garnet–orthopyroxene thermometer based on reversed Al_2O_3 solubility in FeO–Al_2O_3–SiO_2 orthopyroxene. *Am. Mineral.*, 1997. **82**, 345–353.
46. Santosh, M., Tsunogae, Toshiaki., Hisako, S. and Jean, D., Fluid characteristics of retrogressed eclogites and mafic granulites from the Cambrian Gondwana suture zone in southern India. *Contrib. Mineral. Petrol*., 2010, **159**, 349–369.
47. Mukhopadhyay, B. and Bose, M. K., Transitional granulite–eclogite facies metamorphism of basic supracrustal rocks in a shear zone complex in the Precambrian shield of South India. *Mineral. Mag*., 1994, **58**(390), 97–118.
48. Seifert, F., Boron-free kornerupine; a high-pressure phase. *Am. J. Sci.*, 1975, **275**(1), 57–87.
49. Manning, D. A. C. and Pichavant, M., The role of fluorine and boron in the generation of granitic melts. In *High Grade Metamorphism, Migmatites and Melting*, Meeting of the Geochemical Group of the Mineralogical Society of the University of Glasgow, Nantwich, United Kingdom, 1983, pp. 94–109.
50. Robbins, C. R. and Yoder Jr, H. S., Stability relations of dravite, a tourmaline. Carnegie Institution of Washington Yearbook, 1962, vol. 61, pp. 106–108.
51. Grew, E. S., Beryllium in metamorphic environments (emphasis on aluminous compositions). *Rev. Mineral. Geochem*., 2002, **50**(1), 487–549.

ACKNOWLEDGEMENTS. This work is financially supported by a DST-SERB sponsored major research project (P-07-704) to DP. We thank the anonymous reviewers for their valuable comments that helped improve the manuscript.

Received 14 May 2021; revised accepted 31 August 2021

doi: 10.18520/cs/v121/i9/1241-1248